Eur. Phys. J. C 45, 759–769 (2006)
Digital Object Identifier (DOI) 10.1140/epjc/s2005-02451-2

THE EUROPEAN PHYSICAL JOURNAL C

BFKL resummation effects in $\gamma^*\gamma^* \to \rho\rho$

R. Enberg[1,2,a], B. Pire[1], L. Szymanowski[3,4], S. Wallon[5]

[1] CPHT[b], École Polytechnique, 91128 Palaiseau, France
[2] Lawrence Berkeley National Laboratory, Berkeley, CA 94720, USA
[3] Sołtan Institute for Nuclear Studies, Hoża 69, 00-681 Warsaw, Poland
[4] Université de Liège, B4000 Liège, Belgium
[5] LPT[c], Université Paris-Sud, 91405-Orsay, France

Received: 18 August 2005 / Revised version: 5 November 2005 /
Published online: 5 January 2006 – © Springer-Verlag / Società Italiana di Fisica 2006

Abstract. We calculate the leading order BFKL amplitude for the exclusive diffractive process $\gamma^*_{\rm L}(Q_1^2)\gamma^*_{\rm L}(Q_2^2) \to \rho^0_{\rm L}\rho^0_{\rm L}$ in the forward direction, which can be studied in future high energy e^+e^- linear colliders. The resummation effects are very large compared to the fixed-order calculation. We also estimate the next-to-leading logarithmic corrections to the amplitude by using a specific resummation of higher order effects and find a substantial growth with energy, but smaller than in the leading logarithmic approximation.

1 Introduction

The next generation of e^+e^- colliders will offer the possibility of clean testing of QCD dynamics. By selecting events in which two vector mesons are produced with a large rapidity gap in between, through the scattering of two highly virtual photons, one accesses a kinematical regime in which a perturbative approach is justified. If additionally one selects events with comparable photon virtualities, the perturbative Regge dynamics of QCD should dominate and allow the use of resummation techniques of the BFKL [1] type. In this paper we study these effects in the case of the reaction (see Fig. 1)

$$\gamma^*_{\rm L}(q_1)\ \gamma^*_{\rm L}(q_2) \to \rho_{\rm L}(k_1)\ \rho_{\rm L}(k_2) \tag{1}$$

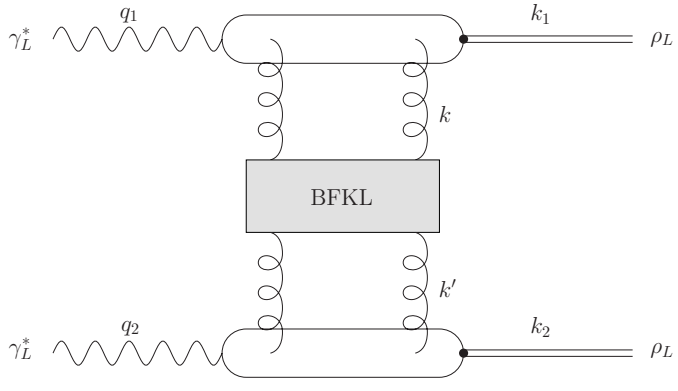

Fig. 1. The process $\gamma^*_{\rm L}(q_1)\ \gamma^*_{\rm L}(q_2) \to \rho^0_{\rm L}(k_1)\ \rho^0_{\rm L}(k_2)$. The box represents the BFKL Green's function, and the t-channel gluons couple to the quark lines in all possible ways

in the forward region, i.e. $-t = -(q_1 - k_1)^2 = -t_{\rm min}$, where the virtualities $Q_1^2 = -q_1^2$, $Q_2^2 = -q_2^2$ of the scattered photons play the role of the hard scales.

This is an interesting process to study, first because the experimental signature is simple: double tagged events in high energy e^+e^- collisions [2], with two longitudinally polarized rho mesons in the final state. The non-zero virtualities of the photons allow studying also the forward region. Second, the theoretical calculation can be performed analytically and gives a simple answer which makes it easy to investigate BFKL effects. This is partly because in the forward region we are studying, the amplitude for transversely polarized photons vanishes identically [3].

No data exist yet for the process (1) at sufficiently high energies, but some experimental data exist for Q_2^2 small [4] which may be analyzed [5] in terms of generalized distribution amplitudes [6]. Related reactions have been calculated, both at the Born level and using BFKL resummation. The similar process with real incoming photons, $\gamma\gamma \to V_1V_2$ and large t where the hard scale is provided by the momentum transfer instead of the photon virtualities, was studied in [7, 8], and the process $\gamma p \to VX$ at large t, has been studied both for heavy [9] and light [10] vector mesons. The advantage of the latter process is that there now exists high quality data from HERA [11], and the BFKL calculations reproduce the measured differential cross sections for longitudinal ρ meson production and for J/ψ production very well, while the Born level calculations do not work so well [9–11]. At the same time the cross section for transversely polarized ρ mesons is not well understood [10].

[a] e-mail: REnberg@lbl.gov
[b] Unité mixte C7644 du CNRS
[c] Unité mixte 8627 du CNRS

In a recent paper [3], the scattering amplitude of the process (1) was calculated in the Born approximation and the feasibility of a dedicated experiment was proved. The production amplitude decreases dramatically with t so that its magnitude at $t = t_{\min}$ dictates the rate of the reaction. In this paper, we report on a calculation of BFKL effects in the leading order approximation at $t = t_{\min}$. We find that the leading logarithmic (LL) BFKL resummation greatly enhances the cross section, as previously observed in other reactions [8,12–14]. In addition, we estimate next-to-leading logarithmic (NLL) effects by the use of the BLM scale fixing prescription [15] supplemented by the resummation scheme of [16–18]. We show that there is still a substantial increase in the cross section compared to fixed-order calculations, but smaller than the LL calculation. It would be interesting to compare our estimates with the ones based on the recently available NLL impact factor for the process $\gamma^* \to V$ of [19] and the NLL BFKL kernel [20].

2 Leading order BFKL forward amplitude

2.1 General expression

In the BFKL framework, the amplitude of the process (1) can be expressed through the inverse Mellin transform with respect to the squared center-of-mass energy s as

$$A(s,t) = \mathrm{i}s \int \frac{\mathrm{d}\omega}{2\pi\mathrm{i}} \mathrm{e}^{\omega Y} f_\omega(r^2), \tag{2}$$

where $t - t_{\min} \sim -r^2$, (r is considered as Euclidean, as is any two-dimensional vector in the following), and Y is the rapidity variable, $Y = \ln(s/s_0)$. The minimum momentum transfer is here given by $t_{\min} \sim Q_1^2 Q_2^2/s$ [3]. In the particular case where $r^2 = 0$, the BFKL Green's function can be easily obtained in momentum space [21]. In this case, the impact representation for $f_\omega(0)$ reads

$$\begin{aligned} f_\omega(0) \; &= \frac{1}{2} \int \frac{\mathrm{d}k^2}{k^3} \frac{\mathrm{d}k'^2}{k'^3} \Phi_1^{ab}(k) \Phi_2^{ab}(k') \\ &\quad \times \int_{-\infty}^{\infty} \mathrm{d}\nu \, \frac{1}{\omega - \omega(\nu)} \left(\frac{k^2}{k'^2} \right)^{\mathrm{i}\nu}, \end{aligned} \tag{3}$$

where the integration over angles has been performed. The functions Φ_i^{ab} are the impact factors describing the coupling of the BFKL pomeron to vertex 1 or 2, and a, b are color indices. The function $\omega(\nu)$ is the BFKL characteristic function which is defined by [1]

$$\omega(\nu) = \bar{\alpha}_\mathrm{s} \chi(\nu), \tag{4}$$

with $\bar{\alpha}_\mathrm{s} \equiv \alpha_\mathrm{s} N_c/\pi$ and

$$\begin{aligned} \chi(\nu) &= 2\psi(1) - \psi\left(\frac{1}{2} + \mathrm{i}\nu\right) - \psi\left(\frac{1}{2} - \mathrm{i}\nu\right), \\ \psi(x) &= \Gamma'(x)/\Gamma(x). \end{aligned} \tag{5}$$

The general solution for arbitrary values of t is more involved [22] and will not be discussed here. We only want to stress that it has a simple expression at the Born level,

$$A = \mathrm{i}s \int \frac{\mathrm{d}^2 k}{k^2 (r-k)^2} \Phi_1^{ab}(k, r-k) \Phi_2^{ab}(k, r-k), \tag{6}$$

which has recently been evaluated in [3]. The special case $r^2 = 0$ of (6) can be readily obtained from (3). This relation will be studied in Sect. 2.2. The impact factor $\gamma_\mathrm{L}^* \to \rho_\mathrm{L}$ is given at $t = t_{\min}$ by [3]

$$\Phi_i^{ab}(k, r=0) = \mathcal{C}^{ab} Q_i \int_0^1 \mathrm{d}z z\bar{z} \phi(z) \left[\frac{1}{m_i^2} - \frac{1}{k^2 + m_i^2} \right], \tag{7}$$

where $m_i^2 = Q_i^2 z\bar{z}$ (with $\bar{z} = 1 - z$), $\phi(z)$ is the distribution amplitude of the meson which is here given by its asymptotic form $\phi(z) = 6z\bar{z}$, and[1]

$$\mathcal{C}^{ab} = \frac{1}{(2\pi)^2} 16\pi^2 \alpha_\mathrm{s} \frac{e}{\sqrt{2}} \frac{\delta^{ab}}{2N_c} f_\rho, \tag{8}$$

where f_ρ is the ρ^0-meson decay constant.

Inserting (7) and (8) in (3) we get

$$\begin{aligned} & f_\omega(r^2 = 0) \\ &= 4\pi\alpha_\mathrm{s}^2 \alpha_\mathrm{em} \frac{N_c^2 - 1}{N_c^2} f_\rho^2 Q_1 Q_2 \int_0^1 \mathrm{d}z_1 z_1 \bar{z}_1 \phi(z_1) \\ &\quad \times \int_0^1 \mathrm{d}z_2 z_2 \bar{z}_2 \phi(z_2) \int_{-\infty}^{\infty} \mathrm{d}\nu \, \frac{1}{\omega - \omega(\nu, n)} \\ &\quad \times \left[\int \frac{\mathrm{d}k^2}{k^3} \left(\frac{1}{m^2} - \frac{1}{k^2 + m^2} \right) k^{2\mathrm{i}\nu} \right] \\ &\quad \times \left[\int \frac{\mathrm{d}k'^2}{k'^3} \left(\frac{1}{m^2} - \frac{1}{k'^2 + m^2} \right) k'^{-2\mathrm{i}\nu} \right]. \end{aligned} \tag{9}$$

Let us denote the expressions in the square brackets by $I(z,\nu)$ and $I(z,-\nu)$ respectively. It is straightforward to put the propagators on a common denominator and show that

$$\begin{aligned} & I(z,\nu) \\ &= -\left(m^2\right)^{-\frac{3}{2}+\mathrm{i}\nu} \Gamma\left(\frac{3}{2} - \mathrm{i}\nu\right) \Gamma\left(-\frac{1}{2} + \mathrm{i}\nu\right) \\ &= -\left(Q_1^2\right)^{-\frac{3}{2}+\mathrm{i}\nu} (z\bar{z})^{-\frac{3}{2}+\mathrm{i}\nu} \Gamma\left(\frac{3}{2} - \mathrm{i}\nu\right) \Gamma\left(-\frac{1}{2} + \mathrm{i}\nu\right). \end{aligned} \tag{10}$$

Next, the z integrals can also be done. We have

$$\begin{aligned} & \int_0^1 \mathrm{d}z \, z\bar{z} \phi(z) I(z,\nu) \\ &= -\left(Q_1^2\right)^{-\frac{3}{2}+\mathrm{i}\nu} \Gamma\left(\frac{3}{2} - \mathrm{i}\nu\right) \Gamma\left(-\frac{1}{2} + \mathrm{i}\nu\right) \end{aligned}$$

[1] The first factor $1/(2\pi)^2$ differs from [3] and comes from the convention for impact factors.

$$\times \int_0^1 \mathrm{d}z\, 6\,(z\bar{z})^{\frac{1}{2}+\mathrm{i}\nu}$$
$$= -6\sqrt{\pi}\, 2^{-2-2\mathrm{i}\nu} \left(Q_1^2\right)^{-\frac{3}{2}+\mathrm{i}\nu} \tag{11}$$
$$\times \Gamma\left(\frac{3}{2}-\mathrm{i}\nu\right)\Gamma\left(-\frac{1}{2}+\mathrm{i}\nu\right)\frac{\Gamma\left(\frac{3}{2}+\mathrm{i}\nu\right)}{\Gamma\left(2+\mathrm{i}\nu\right)},$$

since the integral over z is just the definition of the Euler beta function. Finally this yields the Mellin transform

$$f_\omega(r^2=0) = 9\pi^2\alpha_\mathrm{s}^2\alpha_\mathrm{em}\frac{N_c^2-1}{N_c^2}f_\rho^2 Q_1 Q_2$$
$$\times \int_{-\infty}^{\infty}\mathrm{d}\nu\, \frac{1}{\omega-\omega(\nu)}\left(Q_1^2\right)^{-3/2+\mathrm{i}\nu}\left(Q_2^2\right)^{-3/2-\mathrm{i}\nu} \tag{12}$$
$$\times \frac{\Gamma^2\left(\frac{3}{2}-\mathrm{i}\nu\right)\Gamma^2\left(\frac{3}{2}+\mathrm{i}\nu\right)\Gamma\left(-\frac{1}{2}-\mathrm{i}\nu\right)\Gamma\left(-\frac{1}{2}+\mathrm{i}\nu\right)}{\Gamma\left(2-\mathrm{i}\nu\right)\Gamma\left(2+\mathrm{i}\nu\right)},$$

which immediately leads to the final result for the amplitude (2)

$$A(s,t_\mathrm{min},Q_1,Q_2) = \mathrm{i}s\, 9\pi^2\alpha_\mathrm{s}^2\alpha_\mathrm{em}\frac{N_c^2-1}{N_c^2}f_\rho^2$$
$$\times \frac{1}{(Q_1Q_2)^2}\int_{-\infty}^{\infty}\mathrm{d}\nu\, \mathrm{e}^{\omega(\nu)Y}\left(\frac{Q_1^2}{Q_2^2}\right)^{\mathrm{i}\nu} \tag{13}$$
$$\times \frac{\Gamma^2\left(\frac{3}{2}-\mathrm{i}\nu\right)\Gamma^2\left(\frac{3}{2}+\mathrm{i}\nu\right)\Gamma\left(-\frac{1}{2}-\mathrm{i}\nu\right)\Gamma\left(-\frac{1}{2}+\mathrm{i}\nu\right)}{\Gamma\left(2-\mathrm{i}\nu\right)\Gamma\left(2+\mathrm{i}\nu\right)}.$$

We define $R \equiv Q_1/Q_2$ and write this as

$$A(s,t_\mathrm{min},Q_1,Q_2) = \mathrm{i}s\frac{N_c^2-1}{N_c^2}\frac{9\pi^2\alpha_\mathrm{s}^2\alpha_\mathrm{em}f_\rho^2}{(Q_1Q_2)^2}J(Y,R), \tag{14}$$

with

$$J(Y,R) = \int_{-\infty}^{\infty}\mathrm{d}\nu\, \mathrm{e}^{\omega(\nu)Y}R^{2\mathrm{i}\nu} \tag{15}$$
$$\times \frac{\Gamma^2\left(\frac{3}{2}-\mathrm{i}\nu\right)\Gamma^2\left(\frac{3}{2}+\mathrm{i}\nu\right)\Gamma\left(-\frac{1}{2}-\mathrm{i}\nu\right)\Gamma\left(-\frac{1}{2}+\mathrm{i}\nu\right)}{\Gamma\left(2-\mathrm{i}\nu\right)\Gamma\left(2+\mathrm{i}\nu\right)}.$$

We now want to evaluate the integral J. We have three possibilities at hand:
(i) numerically,
(ii) saddle point approximation and
(iii) sum over residues of poles of the integrand.

The first two methods are used to obtain BFKL results in the rest of this paper.

2.2 Born limit

A very valuable and non-trivial check on the BFKL result as well as the Born result is the fact that in the limit $Y \to 0$ (no evolution) or alternatively $\alpha_\mathrm{s} \to 0$ (the gluons in the ladder do not couple to each other) the BFKL amplitude must reduce to the Born level result. In Appendix A we show, using method (iii) for the evaluation of the integral, that our BFKL result (13) does indeed reduce to the correct Born level results derived in [3], first for the special case $R = 1$ and the DGLAP-like limit $R \gg 1$, and finally for the general case $R \neq 1$. Note that the calculations presented in the Appendix are done in a completely different way than in the Born level calculation in [3], so the agreement is very convincing.

The main results from performing the Born limit are presented in (51), (55) and (58).

2.3 Saddle point approximation of the BFKL amplitude

For $R = 1$ the integrand has a saddle point at $\nu = 0$, but the product of Γ-functions that multiplies the exponential is not very broad. This means the approximation will yield a too large answer. But let us try anyway. The expression multiplying the exponential in the integrand at $\nu = 0$ takes the value $\pi^3/4$, so for the case $Q_1 = Q_2$ we get

$$J(Y,1) \sim \frac{\pi^3\sqrt{\pi}}{4}\frac{\mathrm{e}^{4\ln 2\bar{\alpha}_\mathrm{s}Y}}{\sqrt{14\bar{\alpha}_\mathrm{s}\zeta(3)Y}}, \quad Y \gg 1, \tag{16}$$

so the BFKL amplitude is

$$A(s,t=t_\mathrm{min},Q_1=Q_2=Q) \tag{17}$$
$$\sim \mathrm{i}s\pi^5\sqrt{\pi}\frac{9(N_c^2-1)}{4N_c^2}\frac{\alpha_\mathrm{s}^2\alpha_\mathrm{em}f_\rho^2}{Q^4}\frac{\mathrm{e}^{4\ln 2\bar{\alpha}_\mathrm{s}Y}}{\sqrt{14\bar{\alpha}_\mathrm{s}\zeta(3)Y}}.$$

However, we can do better than this. We can keep the general case $Q_1 \neq Q_2$ with $R \equiv Q_1/Q_2$. The integral is then

$$J(Y,R) = \int_{-\infty}^{\infty}\mathrm{d}\nu\, \mathrm{e}^{\omega(\nu)Y+2\mathrm{i}\nu\ln R}g\left(\frac{1}{2}+\mathrm{i}\nu\right), \tag{18}$$

where $g\left(\gamma=\frac{1}{2}+\mathrm{i}\nu\right)$ was defined in (38). Expanding the exponent to second order we see that the saddle point is shifted:

$$\omega(\nu)Y + 2\mathrm{i}\nu\ln R$$
$$\sim \omega(0)Y + 2\mathrm{i}\ln R\nu + \frac{\omega''(0)Y}{2}\nu^2 \tag{19}$$
$$\sim \frac{\omega''(0)Y}{2}\left(\nu+\frac{2i\ln R}{\omega''(0)Y}\right)^2 + \frac{2\ln^2 R}{\omega''(0)Y} + \omega(0)Y,$$

and we can shift the integration variable accordingly to get a Gaussian integral. The result is now

$$J(Y,R) \sim \frac{\pi^3\sqrt{\pi}}{4}\frac{\mathrm{e}^{4\ln 2\bar{\alpha}_\mathrm{s}Y}}{\sqrt{14\bar{\alpha}_\mathrm{s}\zeta(3)Y}}\exp\left(-\frac{\ln^2 R}{14\bar{\alpha}_\mathrm{s}\zeta(3)Y}\right), \quad Y \gg 1, \tag{20}$$

and

$$A(s,t=t_\mathrm{min},Q_1,Q_2)$$
$$\sim \mathrm{i}s\,\pi^5\sqrt{\pi}\frac{9(N_c^2-1)}{4N_c^2}\frac{\alpha_\mathrm{s}^2\alpha_\mathrm{em}f_\rho^2}{Q_1^2Q_2^2}\frac{\mathrm{e}^{4\ln 2\bar{\alpha}_\mathrm{s}Y}}{\sqrt{14\bar{\alpha}_\mathrm{s}\zeta(3)Y}}$$

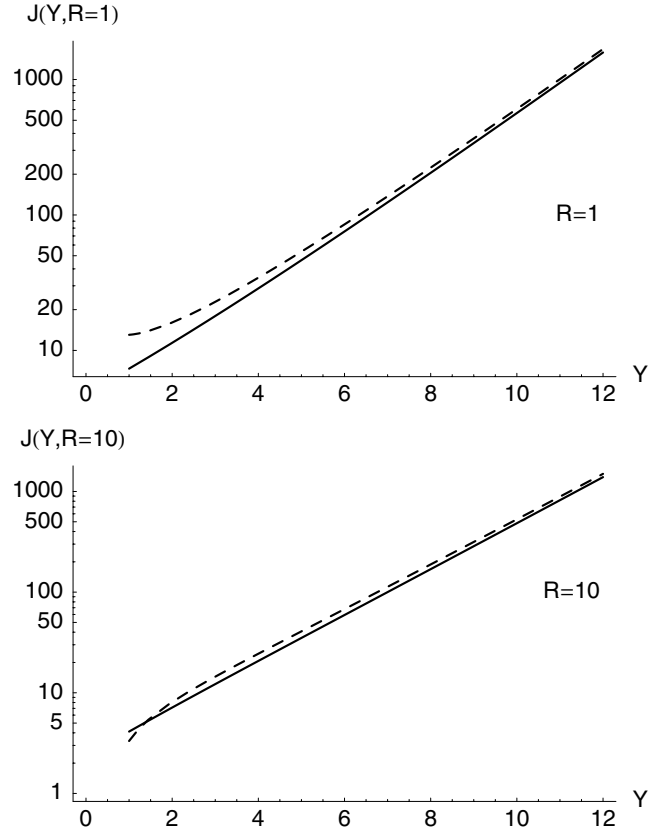

Fig. 2. Exact numerical result (solid line) and saddle point approximation (dashed) to the integral $J(Y, R)$ for $R = 1$ (top) and $R = 10$ (bottom)

$$\times \exp\left(-\frac{\ln^2 R}{14\bar{\alpha}_s\zeta(3)Y}\right). \tag{21}$$

These approximations can be compared to numerical evaluations of the integral for each value of Y. This is illustrated in Fig. 2. We see that the saddle point approximation gives the correct asymptotic behavior for large Y and is less accurate for smaller Y. For $R = 1$ the approximate answer is about 40% too big for $Y \sim 2$ and about 10% too big for $Y \sim 10$. For $R = 10$ the approximation is slightly better. Note that the Linear Collider is likely to test regions with $Y \gtrsim 5$, where the saddle point approximation works relatively well.

2.4 Leading order results

To obtain definite predictions we need to define our parameters. The ρ meson decay constant and the electromagnetic coupling take the values $f_\rho = 216\,\text{MeV}$ [23] and $\alpha_{\text{em}} = 1/137$, respectively. There are furthermore three parameters in the calculation: α_s in the prefactor, which gives the strength of the coupling of the pomeron to the impact factor; $\bar{\alpha}_s$ in the BFKL exponent, which gives the strength of the coupling of the gluons inside the pomeron; and the energy scale of the rapidity Y.

For all cases with a running strong coupling we use a three-loop running $\alpha_s(\mu^2)$ [24] with $\mu^2 = c_\alpha Q_1 Q_2$. Unless otherwise stated, we use this running coupling with $c_\alpha = 1$ in the prefactor of the amplitude.

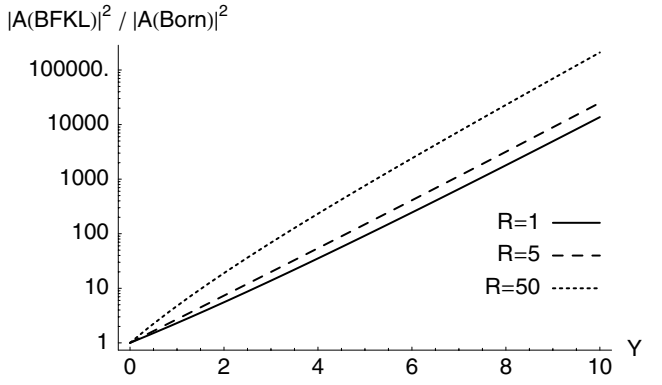

Fig. 3. Ratio of the leading order BFKL cross section $\frac{d\sigma}{dt}\big|_{t_{\min}}$ to the Born level cross section as a function of the rapidity Y, using $\bar{\alpha}_s = 0.2$. The solid curve is for $R = Q_1/Q_2 = 1$, the dashed curve is for $R = 5$, and the dotted curve is for $R = 50$

At LL accuracy, $\bar{\alpha}_s$ is a fixed parameter, i.e., it does not run with the gluon momenta in the BFKL ladder. We choose to, however, let it depend on the given Q_1 and Q_2, which are external to the pomeron but provide a reasonable choice; we thus choose $\bar{\alpha}_s = \frac{N_c}{\pi}\alpha_s(Q_1Q_2)$. The pomeron intercept is determined by $\bar{\alpha}_s$, and it is known to be too large when comparing to HERA data. Our chosen values give quite large pomeron intercepts, but we do not want to artificially suppress the growth by choosing very small values of $\bar{\alpha}_s$. Instead we will see in Sect. 3 that the growth becomes slower when NLL corrections to the BFKL evolution are included.

The rapidity is defined as

$$Y = \ln\left(c_Y \frac{s}{Q_1 Q_2}\right), \tag{22}$$

where c_Y is a constant that is not constrained at LL accuracy. As discussed in [14] this constant is related to the average attained values of $z_{1,2}$ in the process. The authors of [14] chose a very small value $c_Y = 0.01$. We estimate the corresponding effect more conservatively and choose $c_Y = 0.3$ for the cross section predictions shown below (see also [13]).

We will now investigate the sensitivity to these choices. Note that all the results shown in this section have been obtained by numerical evaluation of the integral over ν and not by the saddle point approximation.

We begin by comparing the energy dependence of the BFKL cross section and the Born cross section. Figure 3 shows the ratio of the differential cross sections $d\sigma/dt|_{t=t_{\min}}$ calculated from BFKL and at the Born level, as a function of the rapidity Y for three choices of Q_1 and Q_2, and for a fixed value $\bar{\alpha}_s = 0.2$. There is clearly a strong Y-dependence, as seen from (21). Note that all of the Y-dependence of this ratio comes from the BFKL amplitude, since the Born level result is independent of the energy. Figure 4 shows the same plot but using our "standard" choice of $\bar{\alpha}_s = \frac{N_c}{\pi}\alpha_s(Q_1Q_2)$. The difference between Figs. 3 and 4 serves to illustrate the sensitivity to the choice of $\bar{\alpha}_s$ and shows that using a Q-

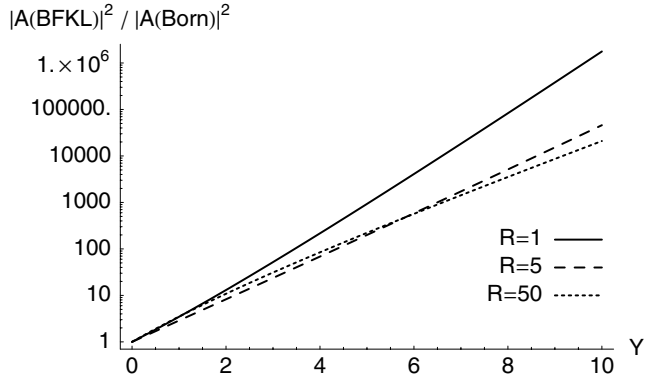

Fig. 4. Same as Fig. 3 but with $\bar{\alpha}_s = \frac{N_c}{\pi}\alpha_s(Q_1Q_2)$, where Q_2 is fixed at $Q_2 = 2\,\mathrm{GeV}$ and $Q_1 = RQ_2$

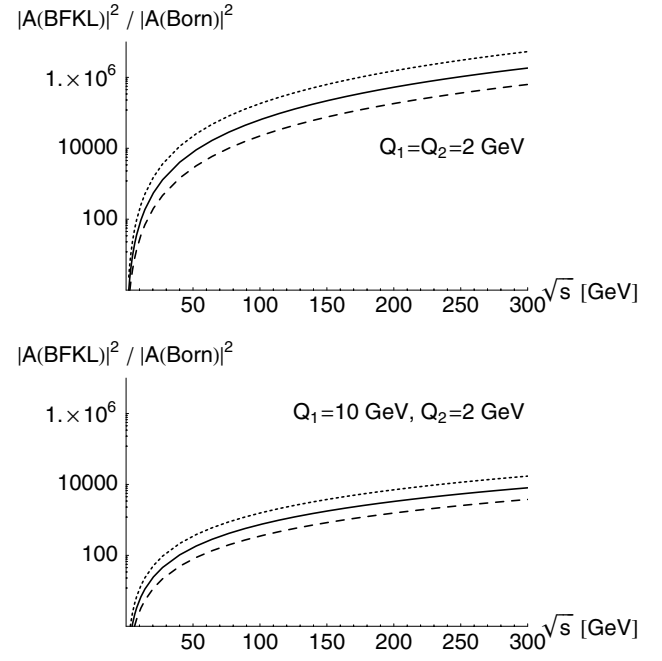

Fig. 5. Ratio of the leading order BFKL cross section $\frac{\mathrm{d}\sigma}{\mathrm{d}t}\big|_{t_{\min}}$ to the Born level cross section as a function of the center-of-mass energy $\sqrt{s}$, for $Q_1 = Q_2 = Q = 2\,\mathrm{GeV}$ (top) and $Q_1 = 10\,\mathrm{GeV}$ and $Q_2 = 2\,\mathrm{GeV}$ (bottom). The different curves in each plot correspond to three different definitions of the rapidity variable, $Y = \ln(c_Y s/(Q_1Q_2))$. The solid curves are for $c_Y = 1$, dashed curves are for $c_Y = 1/2$, and dotted curves are for $c_Y = 2$. The scale of $\bar{\alpha}_s$ is given by $c_\alpha = 1$

dependent coupling for the pomeron decreases the growth with energy for increasing virtualities.

In Fig. 5 we show the same ratios as a function of the center-of-mass energy $\sqrt{s}$ for $Q_1 = Q_2 = 2\,\mathrm{GeV}$ in the left plot and for $Q_1 = 10\,\mathrm{GeV}$, $Q_2 = 2\,\mathrm{GeV}$ in the right plot. The three different curves represent different choices of the energy scale in the definition of Y, corresponding to three different values of the parameter c_Y. This freedom to change the scale introduces an additional uncertainty in the results. In Fig. 6 we show the same kind of plot, but varying instead the parameter c_α in the argument of $\bar{\alpha}_s$ to highlight the uncertainty coming from the choice of scale in α_s. Note that the parameters c_Y and c_α both affect the argument of the BFKL exponential, and thus the energy evolution.

Finally, in Fig. 7 we show the ratio as a function of $Q = Q_1 = Q_2$. Thus we see that the BFKL prediction differs from the Born level prediction in all kinematical variables, which allows testing BFKL dynamics experimentally, and possibly fitting the free parameters.

We have now seen that there are several uncertainties in the calculated amplitude. This has to be kept in mind when viewing the cross section predictions that will follow.

In Fig. 8 we show the differential cross section $\mathrm{d}\sigma/\mathrm{d}t|_{t=t_{\min}}$ as a function of the photon virtuality Q in the symmetric case $R = 1$, i.e. $Q = Q_1 = Q_2$, for three different energies $\sqrt{s}$, and in Fig. 9 we show the same cross section as a function of $\sqrt{s}$ for three different virtualities Q.

These predictions are made with the parameter choices discussed above and contain the corresponding inherent uncertainties. To get some idea of the possible variation in the magnitude of the cross section because of the parameters, we plot in Fig. 10 the cross section for $Q = 2\,\mathrm{GeV}$ for the standard parameter choices, and for two extreme versions, one where we choose new parameters $c'_\alpha = 1/2c_\alpha$, $c'_Y = 2c_Y$ and one with $c'_\alpha = 2\,c_\alpha$, $c'_Y = 1/2\,c_Y$. These curves are plotted in gray and should give some indication of the theoretical uncertainty.

3 Estimation of next-to-leading order effects

The BFKL kernel is known to NLL accuracy [20], and the NLL impact factor for our process has recently been computed [19]. The calculations to obtain the full cross section are difficult, however, and have not yet been performed. It will therefore be interesting to estimate the NLL effects on our calculation. When the cross section is finally computed it may very well be the first complete NLL cross section to be obtained, and it will be very interesting to compare with the estimation presented here.

To estimate higher order effects we thus implement two improvements to the LL BFKL amplitude. First, we use BLM scale fixing [15] for the running of the coupling in the prefactor. Second, we use a renormalization group resummed BFKL kernel, as will be explained below.

In [14] it is shown that for the BFKL calculation of the total $\gamma^*\gamma^*$ cross section, the BLM procedure for choosing the scale leads to $\mu^2 = c_\alpha Q_1 Q_2$ with $c_\alpha = \mathrm{e}^{-5/3}$, and thus to a larger coupling which will increase the cross section. In the process $\gamma^* p \to Vp$ at next-to-leading order [25] the correct scale choice was instead found to be $c_\alpha = \mathrm{e}^{-1/2}$. The use of the BLM procedure in exclusive processes has been further discussed in [26].

An approximate BLM scale for our process is found by using the NLL impact factors computed in [19] and neglecting higher order effects in the BFKL kernel. The BLM procedure then, choosing the scale such that the terms proportional to β_0 vanish, leads to the simple choice $c_\alpha = 1$.

The NLL kernel, taken as it is, is larger than the leading order kernel, and for any reasonable value of α_s it is negative; the pomeron intercept becomes less than one for

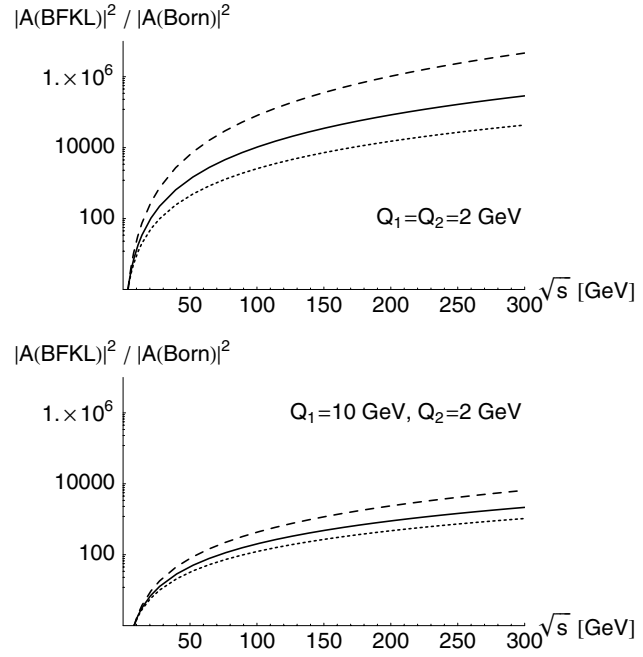

Fig. 6. Same as Fig. 5, but the different curves in each plot correspond instead to three different scale choices in $\bar{\alpha}_s$. The solid curves are for $c_\alpha = 1$, dashed curves are for $c_\alpha = 1/2$, and dotted curves are for $c_\alpha = 2$. The scale of Y is given by the standard $c_Y = 0.3$

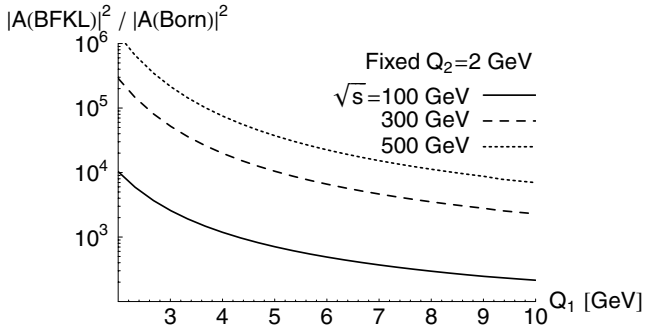

Fig. 7. Ratio of the leading order BFKL cross section $\frac{\mathrm{d}\sigma}{\mathrm{d}t}\big|_{t_{\min}}$ to the Born level cross section as a function of the virtuality Q_1 for fixed $Q_2 = 2\,\mathrm{GeV}$, for three different energies $\sqrt{s}$ and standard scale choices c_α, c_Y as defined in the text

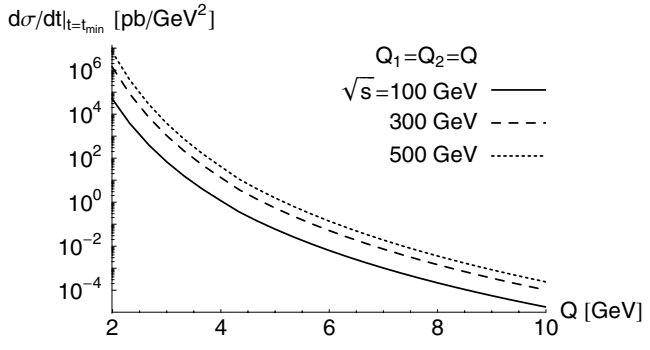

Fig. 8. Differential cross section $\mathrm{d}\sigma/\mathrm{d}t|_{t=t_{\min}}$ as a function of the photon virtuality $Q = Q_1 = Q_2$ for center-of-mass energies $\sqrt{s} = 100\,\mathrm{GeV}$, $300\,\mathrm{GeV}$, and $500\,\mathrm{GeV}$, with standard scale choices as defined in the text

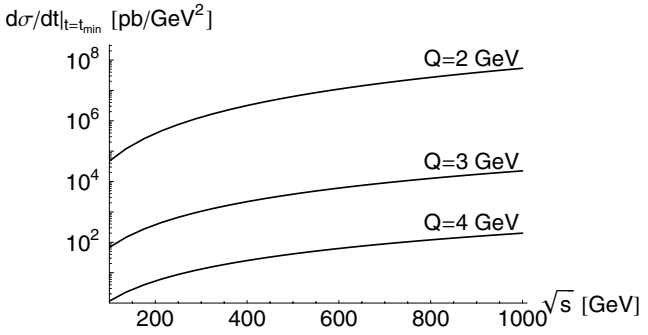

Fig. 9. Differential cross section $\mathrm{d}\sigma/\mathrm{d}t|_{t=t_{\min}}$ as a function of the photon–photon center-of-mass energy $\sqrt{s}$ for photon virtualities $Q = Q_1 = Q_2 = 2\,\mathrm{GeV}$, $3\,\mathrm{GeV}$, and $4\,\mathrm{GeV}$

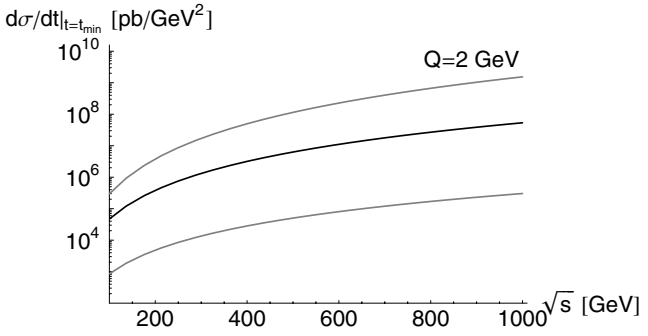

Fig. 10. Differential cross section $\mathrm{d}\sigma/\mathrm{d}t|_{t=t_{\min}}$ for photon virtuality $Q = Q_1 = Q_2 = 2\,\mathrm{GeV}$ for standard parameters c_α, c_Y (black curve) and for new parameters $c'_\alpha = 1/2 c_\alpha$, $c'_Y = 2\,c_Y$ and $c'_\alpha = 2\,c_\alpha$, $c'_Y = 1/2\,c_Y$ (upper resp. lower gray curves)

$\alpha_s \gtrsim 0.15$. Furthermore it has two complex conjugate saddle points which can lead to oscillating cross sections. The perturbative expansion of the BFKL kernel is therefore highly unstable and far from converging. See [16,17,27] for a discussion of these problems.

Different groups have proposed curing the problems of the NLL kernel by certain resummations and methods to stabilize the expansion. In particular some resummation schemes have been proposed [16–18, 28] which lead to modified BFKL kernels[2] $\chi(\gamma, \omega)$ depending on both γ and ω. This form comes about because of a resummation which removes unphysical double logarithms in the DGLAP and "anti-DGLAP" limits where γ is close to 0 or 1 [16], and which resums logarithms from the running of the coupling [17]. This means that when performing the inverse Mellin transform in (2), the position of the pole in the ω plane is determined by the equation

$$\omega = \bar{\alpha}_s \chi(\gamma, \omega). \tag{23}$$

This equation implicitly defines the function $\omega_{\mathrm{NLL}}(\gamma)$ that we need to perform the integral $J(Y, R)$ over $\nu = \mathrm{i}(1/2 - \gamma)$. We therefore estimate the NLL BFKL result by using a resummed BFKL kernel in the BFKL exponential, but we keep the LL form of the solution and the impact factors.

The renormalization group (RG) resummed BFKL kernel of Salam [16] and Ciafaloni et al. [17] is actually a

[2] The discussion is most conveniently performed using the variable $\gamma = \frac{1}{2} + \mathrm{i}\nu$ rather than ν.

resummation of the full NLL kernel, which removes the problems of this kernel. It is however possible to perform such a resummation of the LL kernel, which leads to a result that includes a large part of the corrections coming from the NLL kernel. One such model, based on the general idea of the approach of [16, 17] (more specifically Scheme 4 of [16]), was recently proposed by Khoze et al. [18]. This approach uses a fixed strong coupling in the BFKL kernel which is essential for the approach here. A running coupling in the BFKL kernel radically changes the properties of the solutions, and it is no longer possible to evaluate the ω integral by a simple residue. Therefore we do not pursue it here, although it may be attempted along the lines of [29].

We make one modification to the approach of [18]: they use an asymmetric scale choice in the definition of the rapidity (see [16,17] for a discussion) which was appropriate for their problem under study, but our process is more suited for a symmetric scale choice and we therefore perform the necessary modification. The characteristic function is then expressed as

$$\chi(\gamma,\omega) = \chi_0(\gamma) + \bar{\alpha}_\mathrm{s}\chi_1(\gamma,\omega), \tag{24}$$

where $\chi_0(\gamma) \equiv \chi(\gamma)$ is the usual BFKL function (5). The correction piece $\chi_1(\gamma,\omega)$ is given by

$$\bar{\alpha}_\mathrm{s}\chi_1(\gamma,\omega) = \frac{1+\omega A_1(\omega)}{\gamma+\frac{\omega}{2}} - \frac{1}{\gamma} + \frac{1+\omega A_1(\omega)}{1-\gamma+\frac{\omega}{2}} - \frac{1}{1-\gamma} - \omega\chi_0^{\mathrm{ht}}(\gamma), \tag{25}$$

where χ_0^{ht} is the higher twist part of χ_0,

$$\chi_0^{\mathrm{ht}}(\gamma) = \chi_0(\gamma) - \frac{1}{\gamma} - \frac{1}{1-\gamma} = 2\psi(1) - \psi(1+\gamma) - \psi(2-\gamma). \tag{26}$$

$A_1(\omega)$ is obtained from the Mellin transform of the DGLAP splitting function P_{gg} by

$$\frac{1}{2N_c}P_{gg}(\omega) = \frac{1}{\omega} + A_1(\omega), \tag{27}$$

with

$$A_1(\omega) = -\frac{11}{12} - \frac{n_f}{18} + \left(\frac{67}{36} - \frac{\pi^2}{6}\right)\omega + \mathcal{O}(\omega^2). \tag{28}$$

We will in the following throw away any terms proportional to ω and only keep singular and constant terms. For $n_f = 0$ we then have $A_1(\omega) \simeq -11/12$. It is possible to account for quark loops for $n_f > 0$ by replacing [18]

$$A_1(\omega) \to A_1(\omega) + n_f\left[\frac{\bar{\alpha}_\mathrm{s}}{4N_c^2}\frac{1}{\gamma}P_{gq}(\omega)P_{qg}(\omega) - \frac{1}{3}\right] \simeq -\frac{11}{12} - \frac{7n_f}{18} + \frac{C_F\bar{\alpha}_\mathrm{s}n_f}{6N_c^2\gamma}\left(\frac{1}{\omega} - \frac{11}{6}\right). \tag{29}$$

The characteristic kernel $\omega_{\mathrm{NLL}}(\gamma)$ obtained by solving (23) with $\chi(\gamma,\omega)$ given by (24) is shown both for $n_f = 3$ and $n_f = 0$ in Fig. 11 together with the LL BFKL kernel. An important feature of the kernel (23) is that for $n_f = 0$ it has no pole at $\gamma = 0$. The pole reappears when including the quark loops as shown above. It is also clear that for the resummed kernel both the pomeron intercept and the second derivative at the saddle point are reduced.

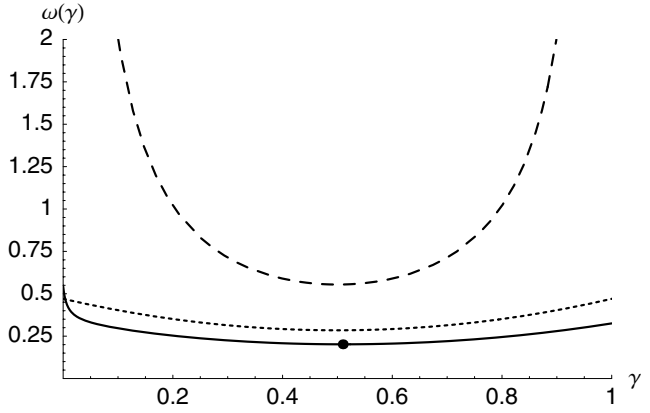

Fig. 11. The characteristic BFKL functions $\omega_{\mathrm{NLL}}(\gamma)$ for the NLL resummed model with $n_f = 3$ (solid line) and $n_f = 0$ (dotted line) and $\omega(\gamma)$ for LL BFKL (dashed line), for a value of $\bar{\alpha}_\mathrm{s} = 0.2$. The dot shows the location of the saddle point of $\omega_{\mathrm{NLL}}(n_f = 3)$, $\gamma_\mathrm{s} = 0.51$, while $\omega(\gamma)$ and $\omega_{\mathrm{NLL}}(n_f = 0)$ have saddle points in $\gamma = 1/2$

To compute the cross section using this model we need to make use of (23) in performing the integral over ν. This is possible to do purely numerically, by solving (23) explicitly for each given value of γ when performing the integral numerically. However, we may obtain some more insight into the properties of the NLL corrections by instead performing the integral by the saddle point method as in Sect. 2.3. We expect the accuracy of the saddle point method to be similar to the LL calculation. For the saddle point calculation we need only compute the position of the saddle point $(\gamma_\mathrm{s}, \omega_\mathrm{s})$, where $\omega_\mathrm{s} \equiv \omega_{\mathrm{NLL}}(\gamma_\mathrm{s})$, and the particular value $\omega_\mathrm{s}'' \equiv \omega_{\mathrm{NLL}}''(\gamma_\mathrm{s})$. These can be obtained explicitly in terms of the partial derivatives of the function $\chi(\gamma,\omega)$ as follows.

The chain rule gives

$$\frac{\mathrm{d}\omega_{\mathrm{NLL}}(\gamma)}{\mathrm{d}\gamma} = \bar{\alpha}_\mathrm{s}\left(\frac{\partial\chi(\gamma,\omega)}{\partial\gamma} + \frac{\partial\chi(\gamma,\omega)}{\partial\omega}\frac{\mathrm{d}\omega_{\mathrm{NLL}}(\gamma)}{\mathrm{d}\gamma}\right), \tag{30}$$

so that the saddle point condition gives

$$\left.\frac{\mathrm{d}\omega_{\mathrm{NLL}}(\gamma)}{\mathrm{d}\gamma}\right|_{\gamma=\gamma_\mathrm{s}} = 0 \quad\Rightarrow\quad \left.\frac{\partial\chi(\gamma,\omega_\mathrm{s})}{\partial\gamma}\right|_{\gamma=\gamma_\mathrm{s}} = 0. \tag{31}$$

We then obtain the second derivative of $\omega_{\mathrm{NLL}}(\gamma)$ (using the saddle point condition)

$$\omega_\mathrm{s}'' = \left.\frac{\mathrm{d}^2\omega_{\mathrm{NLL}}(\gamma)}{\mathrm{d}\gamma^2}\right|_{\gamma=\gamma_\mathrm{s}} = \frac{\bar{\alpha}_\mathrm{s}\left.\frac{\partial^2\chi(\gamma,\omega_\mathrm{s})}{\partial\gamma^2}\right|_{\gamma=\gamma_\mathrm{s}}}{1-\bar{\alpha}_\mathrm{s}\left.\frac{\partial\chi(\gamma_\mathrm{s},\omega)}{\partial\omega}\right|_{\omega=\omega_\mathrm{s}}}. \tag{32}$$

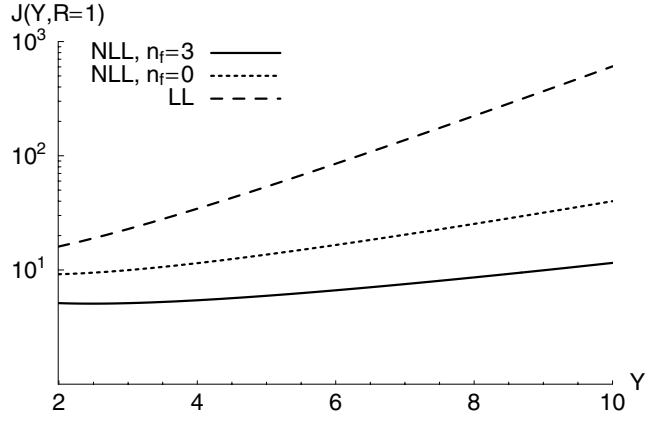

Fig. 12. Saddle point approximation of the integral $J(Y, R = 1)$ for LL BFKL and for the NLL corrected kernel

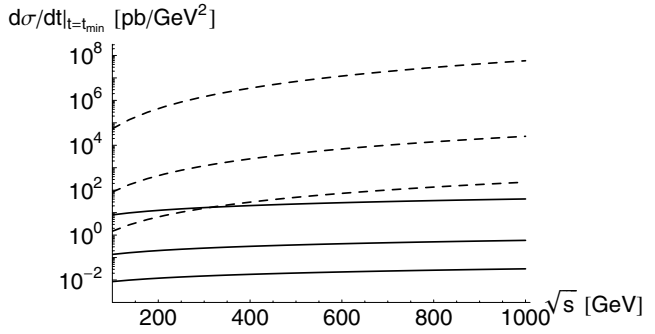

Fig. 13. Cross section for LL BFKL (dashed lines) and for the NLL corrected kernel (solid lines), using $c_Y = 0.3$ and the BLM scale choice $c_\alpha = 1$, for the three cases $Q = Q_1 = Q_2 =$ 2 GeV, 3 GeV and 4 GeV (from top to bottom in the plot)

Finally, to find the saddle point values γ_s, ω_s we must simultaneously solve the equations

$$\begin{cases} \left.\dfrac{\partial\chi(\gamma,\omega_s)}{\partial\gamma}\right|_{\gamma=\gamma_s} = 0, \\ \omega_s = \bar{\alpha}_s\chi(\gamma_s,\omega_s). \end{cases} \tag{33}$$

The symmetric scale choice with $n_f = 0$ gives a kernel symmetric under $\gamma \to 1-\gamma$, so that the saddle point is always located at $\gamma_s = 1/2$. This does not hold for an asymmetric kernel obtained either by the asymmetric scale choice, or, as here, by the inclusion of $n_f > 0$ effects. The saddle point values γ_s, ω_s must then be determined separately for each value of $\bar{\alpha}_s$.

The residue obtained by the integral over ω using the ω-dependent kernel is different from the LL case; we have

$$\operatorname*{Res}_{\omega=\omega_s} \frac{e^{\omega Y}}{\omega - \bar{\alpha}_s\chi(\gamma_s,\omega)} = \frac{e^{\omega_s Y}}{1-\dot{\omega}_s} \tag{34}$$

where we defined the third constant

$$\dot{\omega}_s \equiv \bar{\alpha}_s \left.\frac{\partial\chi(\gamma_s,\omega)}{\partial\omega}\right|_{\omega=\omega_s}. \tag{35}$$

The saddle point evaluation of the integral $J_{\mathrm{NLL}}(Y, R)$ now gives

$$A^{\mathrm{NLL}}(s, t = t_{\min}, Q_1, Q_2) \tag{36}$$
$$\sim \mathrm{i}s\pi^5\sqrt{2\pi}\frac{9(N_c^2-1)}{4N_c^2}\frac{\alpha_s^2\alpha_{\mathrm{em}}f_\rho^2}{Q_1^2Q_2^2}\frac{e^{\omega_s Y}}{\sqrt{\omega_s'' Y}}\frac{\exp\left(-\frac{2\ln^2 R}{\omega_s'' Y}\right)}{1-\dot{\omega}_s}.$$

We show the difference between the energy evolution of the LL kernel and the resummed NLL kernel in Fig. 12. This plot shows the integral $J(Y, R = 1)$ for LL and NLL for a fixed value $\bar{\alpha}_s = 0.2$. The growth with rapidity is strongly reduced by the NLL effects, and the diffusion pattern is also changed. This is quantified by the pomeron intercept $\alpha_{\mathbb{P}} = \omega_s$, which is reduced from $\alpha_{\mathbb{P}} = 0.55$ to $\alpha_{\mathbb{P}} = 0.20$, and by the second derivative ω_s'' of the kernel, which decreases from $\omega_s'' = 28\bar{\alpha}_s\zeta(3) \simeq 6.73$ at the LL level to $\omega_s'' \simeq 2.56$ using the NLL approximation.[3] The overall normalization is also affected by the factor $1/(1-\dot{\omega}_s)$, where in this case $\dot{\omega}_s \simeq -1.51$.

The complete cross section prediction from the NLL modified amplitudes with BLM scale choice is shown in Fig. 13 as a function of the energy. The dashed line shows the LL BFKL result for comparison.

4 Conclusions

Since we expect the linear collider to be able to cover a quite large region in rapidity, experiments will allow us to test the dynamics of pomeron exchange. The Born approximation estimate [3] of this reaction showed that the process $\gamma^*\gamma^* \to \rho\rho$ should be measurable by dedicated experiments at the next linear collider, for virtualities of the photons up to a few GeV^2. The increase of the amplitude that we have obtained when considering BFKL resummation effects is good news for the experimental feasibility of this study. At leading order the growth with energy is very large, but the next-to-leading order effects seem to moderate the growth.

This exclusive diffractive reaction may as anticipated become the best tool to investigate the perturbative picture of the hard pomeron. For example, considering that the full next-to-leading order BFKL calculation of the cross section is likely to appear in the near future [19], measurements of this process would be able to test the impact of the NLL corrections and the various approaches proposed in the literature. Finally, it would also be interesting to pursue this line of research with odderon exchange processes such as $\gamma^*\gamma^* \to \pi^0\pi^0$ or through interference effects in charge asymmetric observables in $\gamma^*\gamma^* \to \pi^+\pi^-\pi^+\pi^-$ [30].

Note added. Shortly after submitting this paper, the paper [31] appeared, containing the full NLL calculation alluded to above, and confirming our LL results. We also note that the BLM scale we obtained under our assumptions in Sect. 3 is not changed if the NLL effects on the BFKL kernel are included.

[3] Note that these values of ω_s and ω_s'' depend on the value of $\bar{\alpha}_s$, so care has to be taken to determine them correctly when using (36).

Acknowledgements. We thank A. Szczurek for discussions on our results. This work is partially supported by the Polish Grant 1 P03B 028 28 and the French–Polish scientific agreement Polonium. L.Sz. is a Visiting Fellow of the Fonds National pour la Recherche Scientifique (Belgium). R.E. would like to thank the Theoretical Physics group at the University of Liège for their hospitality when parts of this work was done.

Appendix A: Born limit

In order to simplify the presentation that follows, we will make this check in two steps. First, we evaluate the integral $J(0,1)$ exactly, that is, in the case that $R = 1$, by picking up all the residues of the integrand in the correct half-plane. Second, the method is generalized to the case where R is arbitrary. In the asymptotic limit $R \gg 1$, the leading contribution can then be easily extracted, as was also done in [3], and further, an explicit twist expansion can be written.

For fixed R, the integral is now just a constant number. Changing to the integration variable $\gamma = \frac{1}{2} + \mathrm{i}\nu$, we get

$$J(0,R) = \frac{1}{R}\int_{1/2-\mathrm{i}\infty}^{1/2+\mathrm{i}\infty} \frac{\mathrm{d}\gamma}{\mathrm{i}}\, g(\gamma), \tag{37}$$

where

$$g(\gamma) \equiv R^{2\gamma}\, g_1(\gamma) \tag{38}$$

with

$$g_1(\gamma) \equiv \frac{\pi^3\gamma(1-\gamma)}{\Gamma(5/2-\gamma)\Gamma(3/2+\gamma)\sin^3(\pi\gamma)} = \frac{f_1(\gamma)}{\sin^3(\pi\gamma)}\,. \tag{39}$$

In the following, we will use the auxiliary functions f and f_1 defined by

$$g(\gamma) \equiv \frac{f(\gamma)}{\sin^3(\pi\gamma)} \equiv R^{2\gamma}\frac{f_1(\gamma)}{\sin^3(\pi\gamma)}\,. \tag{40}$$

The function $g(\gamma)$ obviously has triple poles at all integers as given by the $\sin^3(\pi\gamma)$ factor, except at $\gamma = 0, 1$ where it has double poles.

Let us start with the case $R = 1$. The integration contour (in γ) is parallel to the imaginary axis and crosses the real axis between 0 and 1. The contour can be closed arbitrarily to the right or to the left. We choose to close the contour in the left half-plane and thus to pick up all the poles at $\gamma = -n$, $n = 0, 1, 2, \ldots$

To extract the triple pole residues at $\gamma = -n$, $n = 1, 2, \ldots$ we write $\gamma = x - n$ where $n \in \mathbb{Z}$, $n \neq 0, 1$ and $x \in \mathbb{R}$, $x \ll 1$ so that

$$g(\gamma) = \frac{f(x-n)}{\sin^3\pi(x-n)} \simeq \frac{(-1)^n}{(\pi x)^3}\left[1 + \frac{\pi^2x^2}{2}\right] f(x-n). \tag{41}$$

The residue at $\gamma = -n$ is the residue at $x = 0$, which is by definition for the triple poles

$$\operatorname*{Res}_{\gamma=-n} g(\gamma) \tag{42}$$

$$= \lim_{x\to 0}\frac{1}{2!}\frac{\mathrm{d}^2}{\mathrm{d}x^2}\left(x^3\frac{(-1)^n}{(\pi x)^3}\left[1 + \frac{\pi^2x^2}{2}\right] f(x-n)\right).$$

Taylor expanding $f(x-n)$ around $x = 0$ now easily yields the needed expression:

$$\operatorname*{Res}_{\gamma=-n} g(\gamma) = \frac{(-1)^n}{2\pi^3}\left(f''(-n) + \pi^2 f(-n)\right). \tag{43}$$

This is the first step in the evaluation. We also need a convenient form for $f''(-n)$ that can be summed over n. In order to proceed we rewrite f_1 without any Γ-functions as

$$f_1(\gamma) = \frac{\pi^2\gamma(1-\gamma)\cos\pi\gamma}{(1/2-\gamma)(1/2+\gamma)(3/2-\gamma)}. \tag{44}$$

From this expression, we get after some algebra the derivatives of f_1 up to the second order, at the pole $-n$, in the form

$$\begin{aligned}
f_1(-n) &= (-1)^n\frac{\pi^2}{4}\left(\frac{3}{(2n-1)} + \frac{2}{(2n+1)} + \frac{3}{(2n+3)}\right),\\
f_1'(-n) &= (-1)^n\,\frac{\pi^2}{2}\\
&\quad\times\left(\frac{3}{(2n-1)^2} + \frac{2}{(2n+1)^2} + \frac{3}{(2n+3)^2}\right),\\
f_1''(-n) &= -\pi^2\, f_1(-n) + (-1)^n 2\pi^2\\
&\quad\times\left(\frac{3}{(2n-1)^3} + \frac{2}{(2n+1)^3} + \frac{3}{(2n+3)^3}\right),
\end{aligned} \tag{45}$$

which immediately leads, for $n > 0$, to

$$\operatorname*{Res}_{\gamma_1=-n} g_1(\gamma) = \frac{1}{\pi}\left[\frac{3}{(2n-1)^3} + \frac{2}{(2n+1)^3} + \frac{3}{(2n+3)^3}\right]. \tag{46}$$

The sum over all residues in the left half-plane is therefore related to the definition of the Riemann ζ-function, so

$$\sum_{n=1}^{\infty}\operatorname*{Res}_{\gamma=-n} g_1(\gamma) = \frac{63\zeta(3) - 46}{9\pi}. \tag{47}$$

To evaluate the integral we should also include the double pole of $g_1(\gamma)$ in $\gamma = 0$. Defining

$$h_1(\gamma) = \gamma^2 g_1(\gamma) \tag{48}$$

one gets

$$h_1(0) = \frac{8}{3\pi} \quad\text{and}\quad h_1'(0) = -\frac{8}{9\pi}, \tag{49}$$

and thus the residue is $-8/(9\pi)$. So finally,

$$\sum_{n=0}^{\infty}\operatorname*{Res}_{\gamma=-n} g_1(\gamma) = \frac{7\zeta(3) - 6}{\pi}\,. \tag{50}$$

For our first goal which was to consider $R = 1$, for which $g(\gamma) = g_1(\gamma)$, this sum of residues of g_1 is enough and thus

$J(0,1) = 14\zeta(3) - 12$. The answer for the Born amplitude at $Q_1 = Q_2 = Q$ therefore is

$$A^{\mathrm{Born}}(s, t_{\min}, Q) = \mathrm{i}s \frac{N_c^2 - 1}{N_c^2} \alpha_{\mathrm{s}}^2 \alpha_{\mathrm{em}} f_\rho^2 \frac{9\pi^2}{Q^4} (14\zeta(3) - 12), \quad (51)$$

which is exactly the same as in [3].

Let us now study the general case. Note first that the limits $R \gg 1$ and $R \ll 1$ are of special physical interest, since they correspond to the kinematics typical for deep inelastic scattering on a photon target described through the collinear approximation, i.e. the usual parton model [32]. From (37)–(39), the γ-contour can be closed on the left (respectively right) half-plane for $R > 1$ (respectively $R < 1$). Let us investigate the case $R > 1$. As above for g_1, the integrand g has infinitely many poles: a double pole at $\gamma = 1$ and triple poles at all other integers. Since we are closing the contour in the left half-plane we need only worry about the poles at $\gamma = -|n|$. Using the method that we used above for $R = 1$ gives an expression for the residues at theses poles, and a related series expansion in powers of $1/R^2$ for $J(0,R)$. It consists of a term corresponding to the double pole at 0 (which is leading at large R), plus terms that are suppressed with at least a power $1/R^{2n}$ compared to the $\gamma = 0$ pole. Note that this expansion with respect to $1/R^2$, for fixed values of Q_2, corresponds to a twist expansion. The full resummation of this twist expansion can be performed, as we explain now.

Denoting

$$h(\gamma) = R^{2\gamma} h_1(\gamma) \quad (52)$$

one can readily extract the pole of $g(\gamma)$ at 0 through the relation

$$h'(0) = 2 \ln R h_1(0) + h'(0), \quad (53)$$

which leads to

$$h'(0) = \frac{16}{3\pi} \left(\ln R - \frac{1}{6} \right),$$

and thus to

$$J(0, R \gg 1) \sim \frac{32}{3} \left(\frac{\ln R}{R} - \frac{1}{6R} \right), \quad (54)$$

which, inserted in formula (14) for the amplitude, gives

$$A^{\mathrm{Born}}(s, t_{\min}, Q_1 = R\, Q_2, Q_2) = \mathrm{i}s \frac{N_c^2 - 1}{N_c^2} \alpha_{\mathrm{s}}^2 \alpha_{\mathrm{em}} f_\rho^2 \frac{96\pi^2}{Q_2^4 R^2} \left(\frac{\ln R}{R} - \frac{1}{6R} \right). \quad (55)$$

This is again exactly the result as in [3]. Let us go further. Combining (43) and (38)–(40), one obtains

$$\operatorname*{Res}_{\gamma=-n} g(\gamma) = \operatorname*{Res}_{\gamma=-n} g_1(\gamma) + (-1)^n \frac{2}{\pi^3} \frac{1}{R^{2n}} (\ln^2 R\, f_1(-n) + \ln R\, f_1'(-n)). \quad (56)$$

Using the result (45) for f_1 and f_1', and relating the obtained series to the Li_2 and Li_3 series

$$\mathrm{Li}_2(z) = \sum_{k=0}^{\infty} \frac{z^k}{k^2}, \qquad \mathrm{Li}_3(z) = \sum_{k=0}^{\infty} \frac{z^k}{k^3}, \quad (57)$$

one finally gets, after using (46) and (54),

$$\begin{aligned} J(0,R) &= -6\left(R + \frac{1}{R}\right) - 6\left(R - \frac{1}{R}\right)\ln R - 3\left(R + \frac{1}{R}\right)\ln^2 R \\ &\quad + \left[\frac{3}{R} + 2 + 3R^2\right] \\ &\quad \times \left[\left(\ln\left(1 + \frac{1}{R}\right) - \ln\left(1 - \frac{1}{R}\right)\right)\frac{\ln^2 R}{2}\right. \\ &\quad + \left(\mathrm{Li}_2\left(\frac{1}{R}\right) - \mathrm{Li}_3\left(-\frac{1}{R}\right)\right)\ln R \\ &\quad \left. + \left(\mathrm{Li}_3\left(\frac{1}{R}\right) - \mathrm{Li}_3\left(-\frac{1}{R}\right)\right)\right], \end{aligned} \quad (58)$$

which is in agreement with the result obtained in [3], although the formula given there is expressed in a different way. After some transformations using the Landen relations [33] for Li_2 and Li_3 one finds that the two expressions match. The obtained formula (58) is very convenient to obtain the twist expansion. We illustrate this in the following formula, by giving the first twist correction to the amplitude,

$$\begin{aligned} &A^{\mathrm{Born}}(s, t_{\min}, Q_1 = R\, Q_2, Q_2) \\ &= \mathrm{i}s \frac{N_c^2 - 1}{N_c^2} \alpha_{\mathrm{s}}^2 \alpha_{\mathrm{em}} f_\rho^2 \frac{96\pi^2}{Q_2^4 R^2} \\ &\quad \times \left[\frac{1}{R}\left(\ln R - \frac{1}{6}\right) + \frac{1}{R^3}\left(\frac{2}{5}\ln^2 R + \frac{47}{75}\ln R + \frac{1307}{2250}\right)\right. \\ &\quad \left. + \ldots\right]. \end{aligned} \quad (59)$$

References

1. L.N. Lipatov, Sov. J. Nucl. Phys. **23**, 338 (1976); E.A. Kuraev, L.N. Lipatov, V.S. Fadin, Sov. Phys. JETP **44**, 443 (1976); **45**, 199 (1977); I.I. Balitsky, L.N. Lipatov, Sov. J. Nucl. Phys. **28**, 822 (1978)
2. V.M. Budnev, I.F. Ginzburg, G.V. Meledin, V.G. Serbo, Phys. Rept. **15**, 181 (1974)
3. B. Pire, L. Szymanowski, S. Wallon, Eur. Phys. J. C **44**, 545–558 (2005)
4. P. Achard et al. [L3 Collaboration], Phys. Lett. B **568**, 11 (2003), hep-ex/0305082; B **597**, 26 (2004), hep-ex/0407020; B **615**, 19 (2005), hep-ex/0504016
5. I.V. Anikin, B. Pire, O.V. Teryaev, Phys. Rev. D **69**, 014018 (2004), hep-ph/0307059; hep-ph/0506277
6. M. Diehl, T. Gousset, B. Pire, O. Teryaev, Phys. Rev. Lett. **81**, 1782 (1998), hep-ph/9805380; M. Diehl, T. Gousset, B. Pire, Phys. Rev. D **62**, 073014 (2000), hep-ph/0003233

7. I.F. Ginzburg, S.L. Panfil, V.G. Serbo, Nucl. Phys. B **284**, 685 (1987)
8. J. Kwiecinski, L. Motyka, Phys. Lett. B **438**, 203 (1998), hep-ph/9806260; V.P. Goncalves, W.K. Sauter, hep-ph/0506178
9. J.R. Forshaw, M.G. Ryskin, Z. Phys. C **68**, 137 (1995), hep-ph/9501376; J. Bartels, J.R. Forshaw, H. Lotter, M. Wüsthoff, Phys. Lett. B **375**, 301 (1996), hep-ph/9601201; J.R. Forshaw, G. Poludniowski, Eur. Phys. J. C **26**, 411 (2003), hep-ph/0107068; R. Enberg, L. Motyka, G. Poludniowski, Eur. Phys. J. C **26**, 219 (2002), hep-ph/0207027
10. D.Y. Ivanov, R. Kirschner, A. Schäfer, L. Szymanowski, Phys. Lett. B **478**, 101 (2000) [Erratum B **498**, 295 (2001)], hep-ph/0001255; R. Enberg, J.R. Forshaw, L. Motyka, G. Poludniowski, JHEP **0309**, 008 (2003), hep-ph/0306232; G.G. Poludniowski, R. Enberg, J.R. Forshaw, L. Motyka, JHEP **0312**, 002 (2003), hep-ph/0311017
11. S. Chekanov et al. [ZEUS Collaboration], Eur. Phys. J. C **26**, 389 (2003), hep-ex/0205081; A. Aktas et al. [H1 Collaboration], Phys. Lett. B **568**, 205 (2003), hep-ex/0306013; C. Gwilliam, in Proceedings DIS 2005 (American Institute of Physics, 2005), p. 432
12. J. Bartels, A. De Roeck, H. Lotter, Phys. Lett. B **389**, 742 (1996), hep-ph/9608401; J. Kwiecinski, L. Motyka, Phys. Lett. B **462**, 203 (1999), hep-ph/9905567; Eur. Phys. J. C **18**, 343 (2000), hep-ph/0010029
13. M. Boonekamp, A. De Roeck, C. Royon, S. Wallon, Nucl. Phys. B **555**, 540 (1999), hep-ph/9812523
14. S.J. Brodsky, F. Hautmann, D.E. Soper, Phys. Rev. Lett. **78**, 803 (1997) [Erratum **79**, 3544 (1997)], hep-ph/9610260; Phys. Rev. D **56**, 6957 (1997), hep-ph/9706427
15. S.J. Brodsky, G.P. Lepage, P.B. Mackenzie, Phys. Rev. D **28**, 228 (1983)
16. G.P. Salam, JHEP **9807**, 019 (1998), hep-ph/9806482
17. M. Ciafaloni, D. Colferai, Phys. Lett. B **452**, 372 (1999) hep-ph/9812366; M. Ciafaloni, D. Colferai, G.P. Salam, Phys. Rev. D **60**, 114036 (1999) hep-ph/9905566
18. V.A. Khoze, A.D. Martin, M.G. Ryskin, W.J. Stirling, Phys. Rev. D **70**, 074013 (2004), hep-ph/0406135
19. D.Y. Ivanov, M.I. Kotsky, A. Papa, Eur. Phys. J. C **38**, 195 (2004), hep-ph/0405297
20. V.S. Fadin, L.N. Lipatov, Phys. Lett. B **429**, 127 (1998), hep-ph/9802290; M. Ciafaloni, G. Camici, Phys. Lett. B **430**, 349 (1998), hep-ph/9803389; G. Camici, M. Ciafaloni, Phys. Lett. B **412**, 396 (1997) [Erratum B **417**, 390 (1998)], hep-ph/9707390
21. L.N. Lipatov, in Perturbative Quantum Chromodynamics, edited by A.H. Mueller (World Scientific, Singapore 1986); Phys. Rep. **286**, 131 (1997), hep-ph/9610276
22. L.N. Lipatov, Sov. Phys. JETP **63**, 904 (1986) [Zh. Eksp. Teor. Fiz. **90**, 1536 (1986)]
23. P. Ball, V.M. Braun, Phys. Rev. D **54**, 2182 (1996), hep-ph/9602323
24. S. Bethke, J. Phys. G **26**, R27 (2000), hep-ex/0004021
25. D.Y. Ivanov, L. Szymanowski, G. Krasnikov, JETP Lett. **80**, 226 (2004) [Pisma Zh. Eksp. Teor. Fiz. **80**, 255 (2004)], hep-ph/0407207
26. I.V. Anikin, B. Pire, L. Szymanowski, O.V. Teryaev, S. Wallon, Eur. Phys. J. C **42**, 163 (2005), hep-ph/0411408
27. G.P. Salam, Acta Phys. Polon. B **30**, 3679 (1999), hep-ph/9910492; J.R. Andersen, hep-ph/0507215
28. J. Kwieciński, A.D. Martin, P.J. Sutton, Z. Phys. C **71**, 585 (1996), hep-ph/9602320; B. Andersson, G. Gustafson, H. Kharraziha, J. Samuelsson, Z. Phys. C **71**, 613 (1996); B. Andersson, G. Gustafson, J. Samuelsson, Nucl. Phys. B **467**, 443 (1996)
29. R. Peschanski, C. Royon, L. Schoeffel, Nucl. Phys. B **716**, 401 (2005), hep-ph/0411338
30. P. Hägler et al., Phys. Lett. B **535**, 117 (2002) [Erratum B **540**, 324 (2002)]; Eur. Phys. J. C **26**, 261 (2002)
31. D.Y. Ivanov, A. Papa, hep-ph/0508162
32. V.N. Gribov, L.N. Lipatov, Yad. Fiz. **15**, 781 (1972) [Sov. J. Nucl. Phys. **15**, 438 (1972)]; G. Altarelli, G. Parisi, Nucl. Phys. B **126**, 298 (1977); Y.L. Dokshitzer, Sov. Phys. JETP **46**, 641 (1977) [Zh. Eksp. Teor. Fiz. **73**, 1216 (1977)]
33. See e.g. L. Lewin, Polylogarithms and associated functions (North-Holland, New York 1981)